Appl. Phys. B 81, 265–269 (2005)
DOI: 10.1007/s00340-005-1875-5

Applied Physics B
Lasers and Optics

S.M. KOBTSEV✉
S.V. KUKARIN
N.V. FATEEV
S.V. SMIRNOV

Coherent, polarization and temporal properties of self-frequency shifted solitons generated in polarization-maintaining microstructured fibre

Novosibirsk State University, Pirogova 2, Novosibirsk 630090, Russia

Received: 1 February 2005 / Revised version: 16 April 2005
Published online: 15 July 2005 •

ABSTRACT Coherence of both self-frequency shifted solitons and short-wavelength non-soliton radiation generated in a micro-structure fibre was investigated experimentally for the first time. Their spectral, temporal and polarization characteristics were studied as well. We found the solitons generated in 30-cm-long fibre pumped with 50-fs pulses at 795 nm and 835 nm from Ti:Sapphire oscillator to be coherent, whereas degree of coherence of blue-shifted radiation was amounted to 0.25–0.57 depending on wavelength.

PACS 42.65.Wi; 42.81.Dp

1 Introduction

The effect of continuous shift to the low-frequency domain of ultra-short pulse spectrum observed when increasing the peak power of pulses propagated through a non-linear medium is known as soliton self-frequency shift. This effect makes it possible to generate solitons with tuneable carrier frequency in a broad spectral region by adjusting the power of the pumping source that emits in the spectral region of the anomalous medium dispersion [1, 2]. In the last several years, this effect has been demonstrated in different micro-structure fibres (MF) and tapered fibres (TF) [3–8].

In well-defined instances of this effect, the spectrum of the radiation exiting from MF/TF contains isolated or clearly distinguishable spectral components corresponding to these solitons. These spectral peaks are tuned into the longer-wavelength domain as the pumping power increases, their number being determined by the order of the soliton. This order depends on the following parameters: $N \sim T(\gamma P/|\beta_2|)^{1/2}$ [9], where T and P are duration and power of the pumping pulses, whereas γ and β_2 are the non-linear and the dispersion coefficients of the medium correspondingly. In case the power of the pumping pulses is fixed the degree of manifestation of spectral peaks corresponding to self-frequency shifted solitons (SFSS) is determined by the duration of the pumping pulses [10]: the shorter the pumping pulses, the fewer SFSS are formed and, accordingly, their spectra do not overlap or only overlap slightly. For typical MF/TF the γ parameter amounts to $\sim$ 50–100 W^{-1} km^{-1}, which gives $N = 3$–5 at $P \sim 10$ kW and $\beta_2 \sim 30$ ps^2/km and $T < 40$–50 fs. When the number of SFSS is large ($N > 5$–10) their spectra begin overlapping and finally form a continuous spectrum–continuum that exists in the domain of anomalous medium dispersion. In parallel with this effect (both at small and at large N), there is also the possibility of formation in the region of positive medium dispersion (in the short-wavelength domain) of continuum. The latter one has a different origin and is generated both because of self-modulation of pump radiation and/or because of so-called resonant radiation [11, 12].

At a small number of SFSS ($N \sim 3$) their energies may amount to dozens-per-cent fraction of the pump pulse energy [8], the spectral width of soliton pulses being 25–50 nm [4, 8]. The specific case in which a small number of SFSS is generated together with a continuum in the short-wavelength spectral region is important for a number of applications, in particular for optical comb generation. In f-to-2f scheme [13, 14] one of the soliton radiation frequencies may be used that is separated by an octave from a frequency of short-wavelength non-soliton radiation. In order to employ this generation mode, one has to know the coherence of both soliton components of radiation and those of the short-wavelength continuum.

It is necessary to note that coherent properties of supercontinuum were studied earlier both experimentally [15–18] and theoretically [16–20]. Besides that it was experimentally corroborated that continuum is acceptable in applications where its coherent properties are critical [13, 14, 21]. However, in these investigations no studies of continuum generation modes with strongly expressed soliton components in the long-wavelength spectrum wing were performed, in spite of the fact that these components manifested themselves in various degrees during different stages of continuum spectrum formation and were well identifiable in the temporal representation [19, 20]. In this context it seems important to characterise both experimentally and numerically the degree of coherence of radiation in all spectral areas of continua that contain well-formed long-wavelength spectral peaks corresponding to SFSS.

When radiation with a special spectrum is produced that may be used in optical comb generators, it is obviously preferable to use highly bi-refringent micro-structured fibres

✉ Fax: +7-(3832)-39-72-24, E-mail: kobtsev@lab.nsu.ru

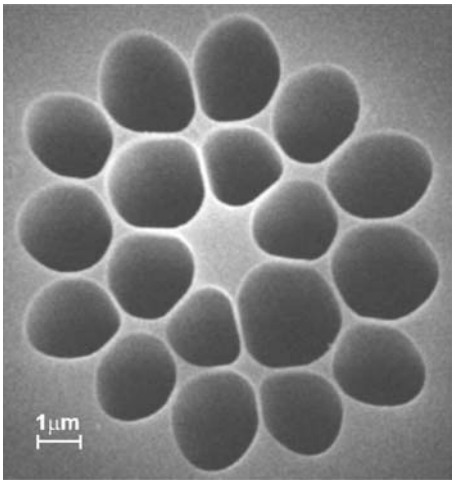

FIGURE 1 Scanning electron micrograph image of MF used for experiments

[22] or dual-core tapered fibres [23] that provide polarised radiation. Polarisation features of transformation of ultra-short pumping pulses in such fibres have been explored earlier [10, 23–25], however these studies were conducted in cases when SFSS in the output spectrum were not isolated or were not clearly identifiable. In this relation it would be interesting to investigate polarisation effects, which are present in when small number of SFSS is generated in bi-refringent microstructured fibre.

In the present work, for the first time were studied the coherent properties of solitons generated in polarisation-maintaining MF with femtosecond pumping, as were their polarisation and temporal parameters experimentally measured.

2 Experiment

In our experiments MF was used. The cross-section of it is shown in Fig. 1. This MF was 30 cm long and had transverse structure close to that of cobweb fibre with an elliptical core of dimensions $1.4 \times 2\mu$ m^2. This MF was pumped at the wavelength of 835 or 795 nm by 50-fs pulses with 100-MHz repetition rate and the average power of 300 mW. The diagram of the experimental set-up is given in Fig. 2. During the experiments interference between the radiation of two successive soliton pulses was registered by an asymmetric Michelson interferometer, the arm difference of the latter providing for the required temporal delay of one of the two pulses. The degree of coherence of the self-frequency shifted solitons was calculated from the visibility of the interference pattern

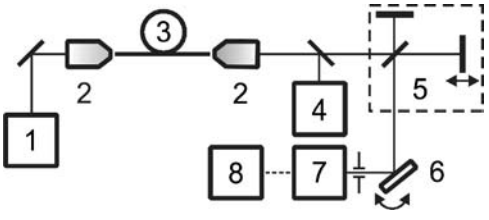

FIGURE 2 Block diagram of the experimental setup: 1-fs Ti:Sapphire laser, 2-micro-objectives, 3-microstructured fiber, 4-optical spectrum analyzer, 5-Michelson interferometer, 6-grating, 7-CCD camera, 8-computer

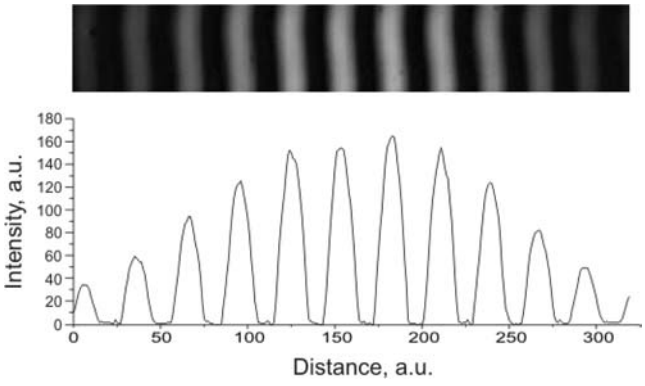

FIGURE 3 Soliton pulse-to-pulse interference pattern and corresponding intensity distribution in the direction perpendicular to the interference fringes

registered on a CCD camera within a given spectral range. Given in Fig. 3 is a typical image of registered interference fringes and corresponding to it intensity distribution of radiation along the direction normal to the fringes. In Figs. 4 and 5 are shown: the radiation spectra at the exit from MF and the measured degrees of coherence of the output radiation within different spectral ranges at pump wavelength of 835 and 795 nm.

The output spectra contain three isolated spectral peaks shifted into the long-wavelength domain relative to the pump wavelength. In the short-wavelength domain one observes a continuous spectrum shown in the log scale in the insets of

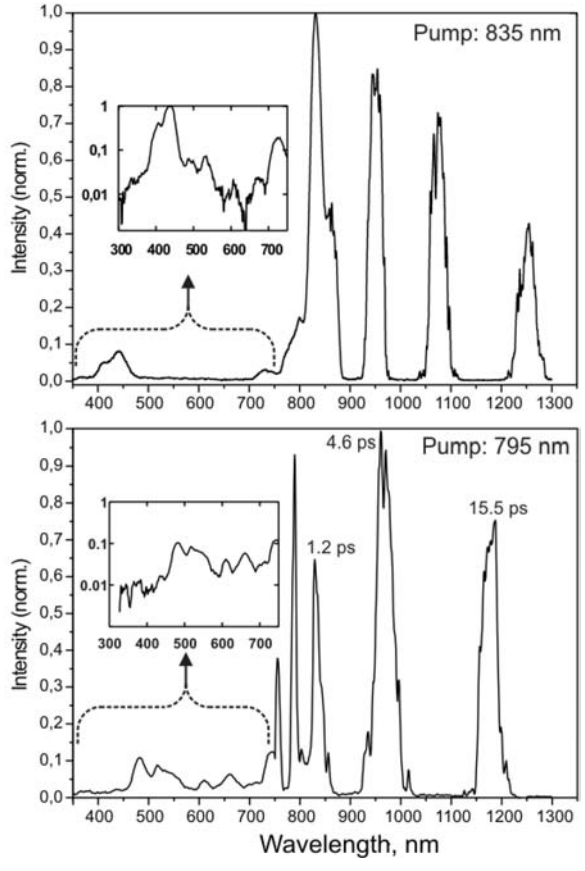

FIGURE 4 The spectrum of radiation at the exit of MF

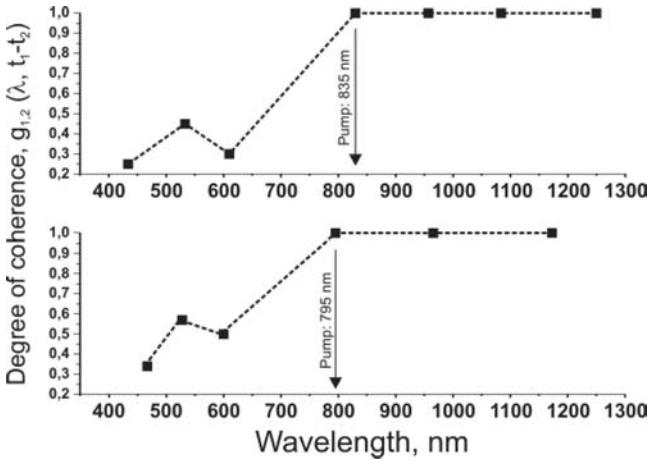

FIGURE 5 The degrees of coherence within different spectrum ranges of radiation at the exit of MF

Fig. 4. At 835-nm-pump this continuum covers the spectral range between 330 nm and the pump radiation wavelength with a gap at 640 nm, which is close to the zero dispersion wavelengths for each of the two eigenpolarization modes of the MF. The frequencies of solitons with spectral peaks at 950 and 1073 nm have spaced by octave 2f components in the central part of the short-wavelength continuum, whereas the 2f components of frequencies of the soliton with peak at 1250 nm are located close to the dip at 640 nm. Theoretically, the f-to-2f scheme can be implemented with frequencies of any of these solitons, since the spectral location of the soliton peaks is easily adjusted by changing the pumping power.

The results of the coherence degree measurements presented in Fig. 5 demonstrate that the degree of coherence of the radiation exiting from MF is the largest for the solitons (as well as for the pump radiation), whereas for the short-wavelength continuum, it is considerably lower than unity and amounts to for different wavelengths of "blue-shifted" radiation: 0.25 (434 nm), 0.45 (531 nm), and 0.3 (609 nm) at pump wavelength of 835 nm and 0.34 (465 nm), 0.57 (527 nm), 0.5 (600 nm) at pump wavelength of 795 nm.

A noticeable difference between the degrees of coherence of SFSS and "blue-shifted" radiation may arise due to a number of reasons. To explore this topic in more detail, we modelled the effect of SFSS generation on the basis of a numerical solution of the generalised non-linear Schrödinger equation. Earlier we used this model to explain generation of SFSS in TF. The results obtained in its framework exhibited good qualitative and quantitative (with respect to the amount of shift in the soliton frequency) agreement with experiment [8]. To study the coherent properties of the radiation some noise was added to the pumping source – one photon with a random phase in each mesh node of the frequency domain [19, 20]. Modelling revealed the presence in the short-wavelength part of the continuum spectrum of a fine structure: oscillations of the spectral power $I(\omega)$ with period $\Delta\omega \sim 0.5$–1 THz, which are brought about by spectra superposition of two or more pulse fragments with close frequencies. Fluctuation of pump radiation power from pulse to pulse leads to a shift of the fine structure of the spectrum (which is confirmed by single-shot experiments [26]). Corresponding relative changes in the spectral power at an arbitrary (fixed) frequency can be close to unity, which leads to considerable reduction of visibility of the interference pattern observed in the experiment. Calculations show that in order to trigger this scenario, it is enough to have pump power fluctuations at the level of $\sim 0.5\%$. Thus, alongside with phase fluctuations, the shift of fine spectral structure can be one of possible reasons of reduced coherence of short-wavelength radiation. This shift may be due both to pump power fluctuations and to the influence of noise on the dynamics of pulse propagation along the fibre and on the spectral broadening, which is also confirmed by numerical calculations. It is pertinent to note that solitons do not contain fine structure in their spectra, this is why, perhaps, the experimentally observed degree of coherence is substantially higher for solitons because it is not subject to the influence of small fluctuations in energy of pumping pulses.

Temporal parameters of the SFSS were studied with the help of an experimental installation analogous to that used in [27]. A small fraction of the pump laser radiation (at 795 nm in this specific experiment) was directed into a delay line (bypassing MF) and then into a non-linear crystal where it was combined with the radiation coming out of MF. At a certain angular position of the crystal and zero delay between the pump pulses and those exiting MF we observed generation at the sum radiation frequency. The wavelength of the maximum of the spectral distribution of the sum-frequency radiation intensity was dependant on the delay of the reference pulse of a Ti:Sapphire laser with respect to the radiation pulse exiting MF. The measurement of temporal delay of the reference pulse and the wavelength of the maximum of the spectral distribution of the sum-frequency radiation intensity was used to obtain the temporal distribution of the relative super-continuum radiation intensity $I(\delta t)$. Temporal resolution of this dependency was determined by the duration of the reference pulse and amounted to 50 fs.

The measured values of the temporal shift of SFSS with respect to the pumping pulses are given in Fig. 4 for the wavelength of pump pulses 795 nm. Delay of soliton pulses with respect to the pumping pulse amounts to 1.2 ps (for the soliton with peak at 834 nm), 4.6 ps (at 966 nm), and 15.5 ps (at 1175 nm).

In order to investigate polarisation properties of self-frequency shifted solitons, we used pumping radiation polarised parallel to the fast or slow axis of the MF elliptic core. In addition, circularly polarised pump radiation was used. In Fig. 6 the spectra at the exit from MF are given for cases when the pump radiation was polarised parallel to either of axes of the MF elliptic core. One of substantial differences between these spectra is the fact that in one of them only blue wing of the short-wavelength continuum is present, whereas in the other — only the green-red wing.

3 Discussion of results

From the viewpoint of metrological applications, the mode in which small number of SFSS is generated together with a continuum in the short-wavelength domain of the spectrum may have advantages compared to the traditionally employed for this purpose broad-bandwidth super-continuum.

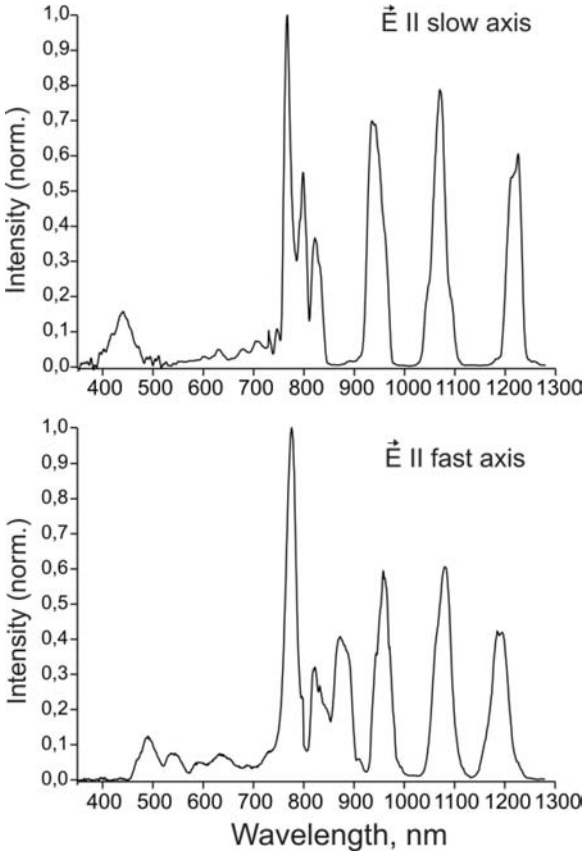

FIGURE 6 Dependence of output spectrum on input polarization orientation for MF of 39 cm long: $\lambda_{pump} = 795$ nm

As was pointed out in [20], the formation of broad-band continuum involves large phase fluctuations, which tend to lower the degree of coherence of the super-continuum components. "Soliton-continuum" mode features advantages of high coherence degree of the soliton components and relatively high spectral density of their radiation, however the coherence degree of the short-wavelength continuum in this mode turned out to be far from the highest in our experimental implementation. It is possible that for maximisation of the degree of coherence of the short-wavelength continuum one has to use even shorter pump pulses. As it was demonstrated in the studies carried out in [17, 19, 20], the coherence degree of continuum components grows when the pumping pulses are shortened.

Temporal distribution of SFSS radiation is correlated with the spectral distribution and contains analogous isolated structures with duration of no more than 0.3 ps. It is worth noting the considerable temporal delays of the soliton pulses with respect to the pump pulse. These delays for different SFSS amount to between $\delta t(\text{ps}) = \Delta\lambda/37$ ps/nm and $\delta t(\text{ps}) = \Delta\lambda/24$ ps/nm, where $\Delta\lambda$ (nm) is the difference of the central wavelengths of the soliton and pump radiation.

Polarisation features of SFSS radiation generated in polarization-maintaining MF turned out in general analogous to those of super-continuum generated in such fibres [10]. Spectra of the output radiation differ for the cases, in which the pump radiation is polarised along the fast and slow axes of the elliptic MF core, whereas the output spectrum in the case of circularly polarised pump radiation is a superposition of the two just-mentioned spectra. The coherence degree of the short-wavelength continuum was measured in both cases of linearly polarised pump; however, the result of these measurements was virtually identical.

4 Conclusions

In the present work, for the first time the coherence degrees of the SFSS radiation were experimentally measured as well as those of components of the simultaneously generated short-wavelength continuum. For solitons the degree of coherence amounted to unity (as it did for the pump radiation), whereas for components of the short-wavelength continuum the degree of coherence was on a lower level and amounted to a pump wavelength of 835/795 nm to 0.25–0.45/0.34–0.57 for different radiation wavelengths within the 430–610 nm range. In this respect, the application of the combined "soliton-continuum" method of broad-band generation for optical combs requires additional studies into the conditions leading to higher coherence degree of components of the short-wavelength continuum. Nevertheless, a set of highly coherent solitons within a relatively broad spectral domain presents a number of independent prospective applications, among these being optical tomography and others.

ACKNOWLEDGEMENTS This work was supported by the INTAS, project No. 03-51-5288.

REFERENCES

1 F.M. Mitshke, L.F. Mollenauer, Opt. Lett. **11**, 659 (1986)
2 J.P. Gordon, Opt. Lett. **11**, 662 (1986)
3 I.G. Cormack, D.T. Reid, W.J. Wadsworth, J.C. Knight, P.St.J. Russel, Electron. Lett. **38**, 167 (2002)
4 D.T. Reid, I.G. Corrmack, W.J. Wadsworth, J.C. Knigth, P.St.J. Russel, J. Modern Opt. **49**, 757 (2002)
5 X. Liu, C. Xu, W.H. Knox, J.K. Chadalia, B.J. Eggleton, S.G. Kossinski, R.S. Windeler, Opt. Lett. **26**, 358 (2001)
6 F.G. Omenetto, A.J. Taylor, M.D. Moores, J. Arriaga, J.C. Knight, W.J. Wadsworth, P.ST.J. Russel, Opt. Lett. **26**, 1158 (2001)
7 B.R. Washburn, S.E. Ralph, P.A. Lacourt, J.M. Dudley, W.T. Rhodes, R.S. Windeler, S. Coen, Electron. Lett. **37**, 1510 (2001)
8 S.M. Kobtsev, S.V. Kukarin, N.V. Fateev, S.V. Smirnov, Laser Phys. **14**, 748 (2004)
9 G.P. Agrawal, *Nolinear Fiber Optics* (Academic, New York, 2001)
10 M. Lehtonen, G. Genty, H. Ludvigsen, M. Kaivola, Appl. Phys. Lett. **82**, 2197 (2003)
11 N. Akhmediev, M.C. Karlsson, Phys. Rev. A **51**, 2602 (1995)
12 W.H. Reeves, D.V. Skryabin, F. Biancalana, J.C. Knight1, P.St.J. Russell, F.G. Omenetto, A. Efimov, A.J. Taylor, Nature **424**, 511 (2003)
13 T.M. Fortier, J. Ye, S.T. Cundiff, R.S. Windeler, Opt. Lett. **27**, 445 (2002)
14 T.M. Fortier, D.J. Jones, J. Ye, S.T. Cundiff, R.S. Windeler, Opt. Lett. **27**, 1436 (2002)
15 M. Bellini, T.W. Haensch, Opt. Lett. **25**, 1049 (2000)
16 M. Nakazawa, K. Tamura, H. Kubota, E. Yoshida, Opt. Fiber Technology **4**, 215 (1998)
17 K.L. Corwin, N.R. Newbury, J.M. Dudley, S. Coen, S.A. Diddams, B.R. Washburn, K. Weber, R.S. Windeler, Appl. Phys. B **77**, 269 (2003)
18 X. Gu, M. Kimmel, A.P. Shreenath, R. Trebino, J.M. Dudley, S. Coen, R.S. Windeler, Opt. Express **11**, 2697 (2003)
19 J.M. Dudley, S. Coen, Opt. Lett. **27**, 1180 (2002)
20 J.M. Dudley, S. Coen, IEEE J. Sel. Top. Quant. El. **8**, 651 (2002)
21 W. Watanabe, Y. Masuda, K. Itoh, Opt. Rev. **6**, 71 (1999)
22 A.M. Zheltikov, *Optics of Microstructure Fibres* (Nauka, Moscow, 2004)

23 S.M. Kobtsev, S.V. Kukarin, N.V. Fateev, Quantum Electronics **33**, 1085 (2003)
24 A. Proulx, J.M. Menard, N. Ho, J.M. Laniel, R. Vallee, C. Pare, Opt. Express **11**, 3338 (2003)
25 Z. Zhu, T.G. Brown, J. Opt. Soc. Am. B **21**, 249 (2004)
26 X. Gu, L. Xu, M. Kimmel, E. Zeek, P. O'Shea, A.P. Shreenath, R. Trebino, R.S. Windeler, Opt. Lett. **27**, 1174 (2002)
27 S.N. Bagaev, V.I. Denisov, V.F. Zahariash, V.M. Klementev, S.M. Kobtsev, I.I. Korel, S.A. Kuznetsov, S.V. Kukarin, V.S. Pivtsov, S.V. Smirnov, N.V. Fateev, Quantum Electronics **34**, 1107 (2004)